

# Extracellular DNA traps are associated with the pathogenesis of TRALI in humans and mice

Grace M. Thomas,<sup>1,2</sup> \*Carla Carbo,<sup>1,2</sup> \*Brian R. Curtis,<sup>3</sup> Kimberly Martinod,<sup>1,4</sup> Irina B. Mazo,<sup>1,2</sup> Daphne Schatzberg,<sup>1</sup> Stephen M. Cifuni,<sup>1</sup> Tobias A. Fuchs,<sup>1,2</sup> Ulrich H. von Andrian,<sup>1,5</sup> John H. Hartwig,<sup>6,7</sup> Richard H. Aster,<sup>3</sup> and Denisa D. Wagner<sup>1,2</sup>

<sup>1</sup>Immune Disease Institute and Program in Cellular and Molecular Medicine, Children's Hospital Boston, Boston, MA; <sup>2</sup>Department of Pediatrics, Harvard Medical School, Boston, MA; <sup>3</sup>Blood Research Institute and Platelet & Neutrophil Immunology Laboratory, BloodCenter of Wisconsin and Department of Medicine, Medical College of Wisconsin, Milwaukee, WI; <sup>4</sup>Graduate Program in Immunology, Division of Medical Sciences, Harvard Medical School, Boston, MA; <sup>5</sup>Department of Microbiology and Immunobiology, Harvard Medical School, Boston, MA; <sup>6</sup>Translational Medicine Division, Department of Medicine, Brigham and Women's Hospital, Boston, MA; and <sup>7</sup>Department of Medicine, Harvard Medical School, Boston, MA

**Transfusion-related acute lung injury (TRALI) is the leading cause of transfusion-related death. The biologic processes contributing to TRALI are poorly understood. All blood products can cause TRALI, and no specific treatment is available. A "2-event model" has been proposed as the trigger. The first event may include surgery, trauma, or infection; the second involves the transfusion of antileukocyte antibodies or bioactive lipids within the blood product. Together, these events induce neutrophil**

**activation in the lungs, causing endothelial damage and capillary leakage. Neutrophils, in response to pathogens or under stress, can release their chromatin coated with granule contents, thus forming neutrophil extracellular traps (NETs). Although protective against infection, these NETs are injurious to tissue. Here we show that NET biomarkers are present in TRALI patients' blood and that NETs are produced in vitro by primed human neutrophils when challenged with anti-HNA-3a antibodies previously implicated**

**in TRALI. NETs are found in alveoli of mice experiencing antibody-mediated TRALI. DNase 1 inhalation prevents their alveolar accumulation and improves arterial oxygen saturation even when administered 90 minutes after TRALI onset. We suggest that NETs form in the lungs during TRALI, contribute to the disease process, and thus could be targeted to prevent or treat TRALI. (*Blood*. 2012;119(26):6335-6343)**

## Introduction

Transfusion-related acute lung injury (TRALI) is a rare but serious complication of blood transfusion that occurs within 6 hours of transfusion and is characterized by hypoxemia, respiratory distress, and pulmonary infiltrates.<sup>1</sup> Over the years, prevention measures have resulted in a significant reduction in cases. However, TRALI is still the leading cause of transfusion-related mortality, and its prevalence is likely underestimated; one study suggested that more than 2% of cardiac surgery patients are affected.<sup>2</sup> Only supportive treatment is available to the patient, including mechanical ventilation and oxygen supplementation. Many of the severe cases have been linked to the presence of antineutrophil antibodies in the transfused product.<sup>3,4</sup> These antibodies bind to the recipients' neutrophils, activate them, and induce sequestration in the pulmonary capillaries, resulting in tissue injury.<sup>5</sup> Activated neutrophils can release neutrophil extracellular traps (NETs)<sup>6</sup> that are composed of DNA fibers decorated with histones and antimicrobial proteins<sup>7</sup> originally contained in the neutrophil granules. The structure and the composition of NETs allow them to trap and prevent the spread of pathogens and also to kill Gram-negative and Gram-positive bacteria, as well as yeast.<sup>6</sup> NET formation follows a specific pattern characterized by histone hypercitrullination,<sup>8</sup> chromatin decondensation, dissolution of the granular and nuclear membranes, and cytolysis.<sup>9</sup> Despite NETs' beneficial antimicrobial

function,<sup>6,10</sup> their formation at the wrong time, in the wrong place, or in the wrong amount can have a negative effect on the host. NETs and their components can be injurious to tissue,<sup>11-13</sup> and they have been shown to contribute to the pathology of several inflammatory diseases.<sup>12-17</sup>

The purpose of this study was to determine whether NETs are formed in patients with TRALI and contribute to TRALI in a mouse model. Antibodies implicated in severe TRALI and directed against the human neutrophil alloantigen-3a (HNA-3a) have been identified and shown to bind to choline transporter-like protein 2 (CTL-2) on the recipients' neutrophils.<sup>18,19</sup> We evaluated whether the antibody enhances NET formation in vitro in human neutrophils expressing HNA-3a. We also investigated whether NETs were formed in the lungs of mice with TRALI.

## Methods

### Human samples

Blood samples from 5 patients with TRALI, 3 blood donors whose plasma caused TRALI, and 11 healthy control subjects were included in the study. TRALI was diagnosed in patients according to the international consensus definition.<sup>1</sup> Studies involving human subjects were approved by the

Submitted January 20, 2012; accepted May 10, 2012. Prepublished online as *Blood* First Edition paper, May 17, 2012; DOI 10.1182/blood-2012-01-405183.

\*C.C. and B.R.C. contributed equally to this study.

The online version of this article contains a data supplement.

The publication costs of this article were defrayed in part by page charge payment. Therefore, and solely to indicate this fact, this article is hereby marked "advertisement" in accordance with 18 USC section 1734.

© 2012 by The American Society of Hematology

Institutional Review Boards of the Immune Disease Institute and the BloodCenter of Wisconsin. The investigation conforms to the principles outlined in the Declaration of Helsinki.

### Experimental mice

Experiments were performed using 8- to 10-week-old BALB/c male mice purchased from The Jackson Laboratory. All mice were housed in the animal facility at the Immune Disease Institute. Experimental procedures performed on the mice were approved by the Animal Care and Use Committee of the Immune Disease Institute.

### Two-event TRALI model

The model was adapted from Looney et al.<sup>20</sup> Male BALB/c mice (8 to 10 weeks old) were primed with an intraperitoneal injection of lipopolysaccharide (LPS; 0.1 or 0.5 mg/kg, as indicated in the text) 24 hours before challenge with anti-H-2K<sup>d</sup> mAb (clone 34-1-2s, 1 mg/kg) or isotype control injected retro-orbitally. In experiments involving DNase 1 treatment, mice that were injected with both LPS and the anti-H-2K<sup>d</sup> mAb received intranasal DNase 1 (Pulmozyme, Genentech; 50 µg/mouse, 1 µg/µL) 10 minutes before or 90 minutes after antibody injection. Control TRALI mice were injected with 50 µL of the DNase 1 vehicle-buffer in DNase 1 experiments. Blood collection, lung harvesting, and arterial oxygen saturation measurements were all performed 2 hours after antibody injection. No event of TRALI-related death was recorded under these conditions in any of the treated mice.

### Body temperature measurements

Rectal temperatures were measured as an indicator of shock-like condition 2 hours after anti-H-2K<sup>d</sup> infusion using a rectal temperature probe (MouseOx Plus system; STARR Life Sciences) connected to a PowerLab data acquisition system (ADInstruments).

### Antibody preparation

Anti-HNA-3a antibodies from blood donors whose plasma induced TRALI in patients and control IgG from a control donor were purified using a protein G-Sepharose column (GE Healthcare). F(ab')<sub>2</sub> fragments were generated from purified anti-HNA-3a antibody using the F(ab')<sub>2</sub> Preparation Kit (Pierce Chemical). Quality of the obtained F(ab')<sub>2</sub> was verified after electrophoresis on SDS-PAGE gel and silver stain. Anti-H-2K<sup>d</sup> antibodies were purified from the hybridoma 34-1-2s with a protein A-Sepharose column (GE Healthcare). The antibody preparation was then dialyzed and tested by electrophoresis on SDS-PAGE gel followed by silver stain, dot-blot, and flow cytometry.

### Blood counts

Mouse peripheral blood counts were measured from EDTA-anticoagulated blood with a Hemavet 950 veterinary hematology analyzer (Drew Scientific). This blood counter uses 2 different currents to analyze the cells. A low voltage current determines the volume and the number of cells (Coulter Impedance principle), and a high voltage current that passes through the cells generates information on their internal structure, such as nucleus, fluid, granules, and vacuoles.

### Bronchoalveolar lavages

Mice were killed and intubated with a 24-gauge cannula after their tracheas were surgically isolated. The lungs were flushed 3 times with 0.8 mL of sterile PBS. Bronchoalveolar lavage fluids were centrifuged for 5 minutes at 800g. Protein concentration was quantified in the supernatant using the bicinchoninic acid method.

### Measurements of blood arterial oxygen saturation

Blood arterial oxygen saturation was recorded 2 hours after anti-H-2K<sup>d</sup> antibody injection, using a small rodent oxymeter sensor (Mouse<sup>OX</sup>; STARR Life Sciences) mounted on the collar of each tested mouse. The

2-hour end point was used as per the model published by Looney et al in 2009.<sup>20-22</sup>

### Human neutrophils

Human neutrophils were isolated from blood by dextran sedimentation followed by Ficoll-Hypaque gradient centrifugation. Briefly, 10 mL of blood containing EDTA was diluted in 10 mL of 3% Dextran and sedimented for 20 minutes. The leukocyte-rich, erythrocyte-poor upper fraction was then centrifuged at 500g for 10 minutes to pellet the leukocytes. Leukocytes were layered with Ficoll-Hypaque and separated under centrifugation for 30 minutes at 400g. Hypotonic red blood cell lysis was then performed to eliminate the residual erythrocytes and the neutrophils were washed in PBS and resuspended in RPMI containing 10mM HEPES. Neutrophil purity was routinely more than 98% as assessed by differential cell count after modified Wright-Giemsa staining. Blood samples from different blood donors were selected for the ability of their neutrophils to agglutinate in response to plasma containing anti-HNA-3a antibodies.

### Granulocyte agglutination test

The granulocyte agglutination test was performed as previously described.<sup>11</sup> The agglutination was observed microscopically, and the degree of agglutination was graded from – (negative), ± (weak) or + (positive).

### NET quantification

The protocol was adapted from the method of Kessenbrock et al.<sup>14</sup> HNA-3a–positive neutrophils were allowed to adhere on a 96-well plastic plate for 30 minutes at 37°C. The neutrophils were then primed with 5 ng/mL TNF-α and incubated with 33nM (equivalent of 5 µg/mL) of control IgG purified from healthy volunteer blood (control antibody), anti-HNA-3a whole IgG purified from 2 blood donors whose plasma induced TRALI (Ab1 or Ab2), anti-CD11a IgG (anti CD11a Ab), F(ab')<sub>2</sub> fragments (equivalent to 3.66 µg/mL) prepared from a purified anti-HNA-3a IgG preparation from a blood donor whose plasma induced TRALI (F(ab')<sub>2</sub>), or with 25nM phorbol 12-myristate 13-acetate (PMA; positive control). After a 180-minute incubation, cells were fixed with 2% paraformaldehyde, and the DNA was stained using Hoechst 33342. The released DNA was visualized by fluorescence microscopy, and percentage of cells making NETs was quantified from 7 to 9 nonoverlapping fields in 3 wells for each treatment.

### Extracellular DNA and nucleosome quantification in plasma

Plasma DNA and extracellular nucleosomes were quantified according to manufacturer's instructions using commercially available quantification kits (from Invitrogen and Roche, respectively).

### MPO activity determination

Mouse lungs were weighed, blended in 50mM potassium phosphate buffer, centrifuged, resuspended, and sonicated in potassium phosphate buffer supplemented with 50mM hexadecyltrimethyl ammonium bromide. After centrifugation of the cell lysates, myeloperoxidase (MPO) activity was assessed in the supernatant by adding tetramethylbenzidine and absorbance reading at 450 nm after stopping the reaction with sulfuric acid. For MPO quantification in mouse plasma, plasma was diluted in potassium phosphate buffer supplemented with 50mM hexadecyltrimethyl ammonium bromide, and MPO activity was measured as previously described for lung tissue. MPO was quantified in human samples using a commercially available ELISA activity assay kit (Invitrogen) according to manufacturer instructions.

### Immunohistology

Mouse lungs were fixed by intratracheal infusion of zinc fixative, and then excised and bathed in zinc fixative for 2 hours at 4°C. Intratracheal inflation of the lung allowed us to conserve the 3-dimensional alveolar structure. The lungs were then washed in PBS, embedded, and cryosectioned into 10-µm or 50-µm sections for widefield and multiphoton fluorescence microscopy,

respectively. Sections were incubated with zinc fixative for 15 minutes, washed in PBS, and permeabilized (0.1% Triton X-100, 0.1% sodium citrate) on ice. After washing and blocking (3% BSA), the sections were incubated for 2 to 16 hours at 4°C in 0.3% BSA with 1  $\mu\text{g}/\text{mL}$  anti-mouse Gr-1 (Ly-6G/C, clone RB6-8C5, BD Biosciences), 0.3  $\mu\text{g}/\text{mL}$  rabbit antihistone H3Cit (citruiline 2, 8, 17; ab5103, Abcam), or sheep anti-mouse VWF (1:50 dilution of IgG fraction, ab11713, Abcam). Sections were then washed and incubated with the following Alexa-conjugated secondary antibodies (Invitrogen) in 0.3% BSA: Alexa 555-goat anti-rat IgG (2  $\mu\text{g}/\text{mL}$ ), Alexa 488-donkey anti-rabbit IgG (1.5  $\mu\text{g}/\text{mL}$ ), or Alexa 568-donkey anti-sheep IgG (2  $\mu\text{g}/\text{mL}$ ) for 2 to 4 hours at room temperature. DNA was labeled with 1  $\mu\text{g}/\text{mL}$  Hoechst 33342 (Invitrogen) before mounting. Fluorescent images were acquired using a Zeiss Axiovert 200 inverted fluorescence microscope in conjunction with a Zeiss Axiocam MRm monochromatic CCD camera and analyzed with Axiovision 4.6 software (Zeiss) or using a Zeiss Axioplan upright fluorescence microscope in conjunction with a Hamamatsu CCD Camera coupled to an image intensifier (videoscope), and analyzed with Slidebook 5.0 software (Intelligent Imaging Innovations).

### Multiphoton fluorescence microscopy

We used a custom-built Ultima system from Prairie Technologies. The microscope was equipped with a water immersion objective (20 $\times$ /0.95 numeric aperture), a laser scanning microscopy device, which incorporates a computer with beam-conditioning equipment, and a scanhead connected to an Olympus IX50 microscope stand. For multiphoton excitation and second-harmonic generation, a MaiTai Ti:sapphire laser (Spectra-Physics) was tuned to 1000 nm to balance excitations of various fluorescent probes used. Emitted light and second-harmonic signals were detected through 455/70-nm, 525/50-nm and 590/50-nm band-pass filters with nondescanned detectors for the generation of 3-color images. Sequences of image stacks were transformed into volume-rendered videos with Volocity 5.2 (Improvision) or Imaris 7.2 (Bitplane Scientific Solutions) software. Only 50- $\mu\text{m}$ -thick lung tissue cryosections were analyzed.

### Transmission electron microscopy

Mouse lungs were fixed by intratracheal infusion of 1.5% formaldehyde/1.5% glutaraldehyde in sodium cacodylate buffer (pH 7.35), excised and bathed in the same solution for 2 hours at 4°C. The fixed lungs were sliced into 0.5-mm sections; the sections were washed extensively in distilled water, frozen on a liquid-helium cooled copper block, freeze-dried at  $-80^\circ\text{C}$ , and coated with 2 nm of platinum at a 45-degree angle with rotation and 10 nm of carbon without rotation. Tissue was removed from the metal casting using bleach (Austin A-1-5.25% sodium hypochlorite), washed and picked up on formvar-coated 200 mesh copper grids. Grids were photographed in a JEOL-1200 EX electron microscope at 100 kV.

### Statistical analyses

Statistical significance for nonparametric distributions (mouse and human samples) was assessed with the 2-tailed Mann-Whitney test for 2 groups. The 1-way ANOVA test with Bonferroni posttest was used for *in vitro* studies (NET quantifications). We used GraphPad Prism Version 4.0 software for all analyses.

## Results

### Antineutrophil antibody linked to TRALI promotes NET formation *in vitro*

Because anti-HNA-3a antibodies cause the most severe TRALI,<sup>3,18,19</sup> we tested whether such antibodies could promote NET formation by human neutrophils. IgG were purified from 2 blood donors with anti-HNA-3a antibodies whose plasma caused a TRALI reaction in patients and control IgG were purified from a control donor's plasma. Neutrophils positive for the HNA-3a antigen were isolated from healthy volunteers' blood and primed with 5 ng/mL of TNF- $\alpha$ , an LPS-induced

cytokine. The neutrophils were then incubated with 5  $\mu\text{g}/\text{mL}$  of either anti-HNA-3a IgG or control IgG for 180 minutes and compared with the effect of PMA to quantify their capacity to induce NETs. Using fluorescence microscopy, we observed that TNF- $\alpha$ -primed neutrophils formed significantly more NETs upon incubation with the 2 sources of anti-HNA-3a antibodies (Ab1 and Ab2) compared with neutrophils incubated with control IgG (Figure 1A-B). Moreover, a majority of the neutrophils treated with the anti-HNA-3a antibody lost their lobulated nucleus morphology. This delobulation was associated with a larger nucleus area (Figure 1B), which is a typical early event in the formation of NETs.<sup>23</sup>

Because Fc $\gamma$ R engagement has been shown to be linked to robust ROS generation<sup>24</sup> and ROS generation promotes NET formation,<sup>9</sup> we hypothesized that Fc $\gamma$ R engagement by antineutrophil antibodies could promote NETosis. To test this hypothesis, F(ab')<sub>2</sub> fragments were prepared from anti-HNA-3a IgG purified from a blood donor whose plasma induced TRALI (Ab1). The incubation of anti-HNA-3a F(ab')<sub>2</sub> fragments with TNF- $\alpha$ -primed neutrophils did not induce NETs generation to a greater extent than TNF- $\alpha$  alone (Figure 1C). As a second approach, we blocked the Fc $\gamma$ RIIa (CD32)-binding sites on human neutrophils with the IV.3 antibody<sup>25</sup> before TNF- $\alpha$  and anti-HNA-3a antibody treatment. The increase in NETosis was no longer observed after anti-HNA-3a antibody (Ab1, Ab2) stimulation (supplemental Figure 1, available on the *Blood* Web site; see the Supplemental Materials link at the top of the online article). Together, these results indicate that anti-HNA-3a antibodies trigger neutrophil activation, ultimately leading to NET generation likely through a Fc $\gamma$ RIIa-dependent process.

### NET biomarkers can be detected in the bloodstream of patients with TRALI

To determine whether NETs are formed in humans during TRALI, the presence of NET degradation products was assessed in the blood of patients with documented TRALI. For that purpose, serum samples from 6 healthy volunteers and from 5 patients who developed pulmonary insufficiency within 1 to 6 hours of transfusion and were diagnosed with TRALI (supplemental Table 1)<sup>1</sup> were blindly screened. A significant increase in circulating DNA and nucleosome levels was detected in the TRALI patients compared with the healthy subjects (Table 1). Based on the increase in concentration of these markers, samples that originated from TRALI patients versus control persons were correctly identified. Blood donors that induced TRALI (supplemental Table 2) did not contain excessive DNA or nucleosomes compared with healthy control subjects, indicating that NETs formed in the recipients after transfusion (supplemental Table 3). Even though the increase in circulating levels of DNA and nucleosomes cannot be exclusively attributed to NET formation, the tendency for serum MPO to increase in TRALI patients probably reflects neutrophil activation.

### Antibody-mediated TRALI causes NET formation in the lungs of mice

We next used a previously established *in vivo* model of antibody-induced TRALI in mice.<sup>20,21,26</sup> In this 2-event model, BALB/c mice are injected intraperitoneally with a low dose of LPS (0.1-0.5 mg/kg) and 24 hours later are infused with an anti-MHC class I monoclonal antibody (anti-H-2K<sup>d</sup>). Two hours later, we measured arterial blood oxygen saturation to document lung function. The mice were then killed and lung injury markers<sup>26</sup> quantified (supplemental Figure 2). As observed in blood from TRALI



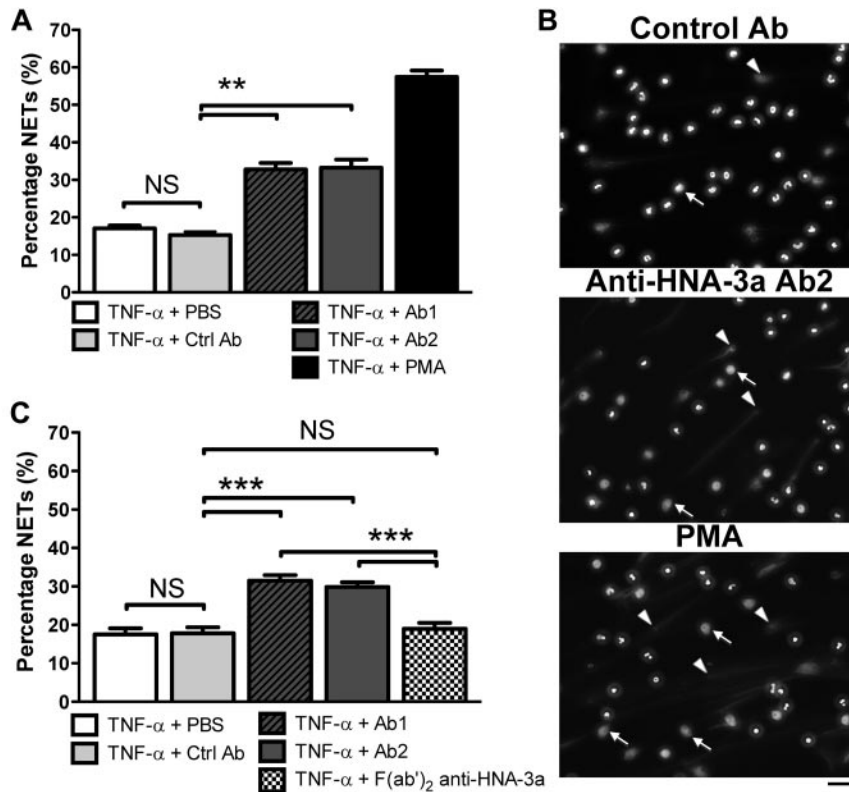


**Figure 1. Effect of anti-HNA-3a antibody on NET formation by human neutrophils.** (A) Quantification of NETs after anti-HNA-3a antibody treatment by fluorescence microscopy analysis. HNA-3a-positive neutrophils primed with TNF- $\alpha$  were incubated for 180 minutes with PBS (TNF- $\alpha$  + PBS), control IgG purified from healthy volunteer plasma (TNF- $\alpha$  + Ctrl Ab), anti-HNA-3a antibody purified from 2 donors whose plasma induced TRALI (TNF- $\alpha$  + Ab1 and TNF- $\alpha$  + Ab2), or 25nM PMA as a positive control (TNF- $\alpha$  + PMA). DNA release was visualized after DNA staining with Hoechst 33342. The experiment was independently performed 9 times. Bars represent mean  $\pm$  SEM.  $**P < .01$ . (B) Examples of the fluorescence images quantified in panel A. White arrowheads indicate selected cells forming NETs; and white arrows, examples of delobulated (large) neutrophil nuclei. Their presence indicates nuclear decondensation, an early step in NETosis. Scale bar represents 50  $\mu$ m. (C) Quantification of NETs after anti-HNA-3a F(ab')<sub>2</sub> fragment treatment by fluorescence microscopy analysis. HNA-3a-positive neutrophils were incubated and analyzed in the same conditions as in panel A but were also treated with anti-HNA-3a F(ab')<sub>2</sub> fragments (TNF- $\alpha$  + F(ab')<sub>2</sub> anti-HNA-3a). The experiment was independently performed 3 times. Bars represent means  $\pm$  SEM.  $***P < .005$ . NS indicates not significant.

patients, a significant increase (1.3- to 3.6-fold) in the concentration of NET biomarkers, such as DNA, nucleosomes, and MPO, was detected in the plasma of mice with TRALI compared with mice that were challenged only with LPS (Figure 2). Besides endothelial cells, monocytes, and platelets,<sup>20,26,27</sup> neutrophils are essential in the pathophysiology of TRALI.<sup>3,26</sup> Their recruitment to lung tissue combined with their activation induced by antibody transfusion<sup>20</sup> let us hypothesize that NETs are formed in the lungs of mice during TRALI. We used transmission electron microscopy to address this question (Figure 3). This technique allowed us to

detect a fibrous mesh coating the alveoli within the airspace in the TRALI group (Figure 3B,D), but such a mesh was not detected in control mice (Figure 3A). Because fibrin and DNA cannot be distinguished by electron microscopy<sup>28</sup> and because DNase 1 cleaves DNA but not fibrin,<sup>29</sup> LPS-primed mice were treated with intranasal DNase 1 administration 10 minutes before antibody injection. Two hours after anti-H-2K<sup>d</sup> mAb challenge, no fibrous material could be detected in the DNase 1-treated alveoli (Figure 3C); thus, DNA was the basis of the fibrous mesh in the alveoli of mice with TRALI. These results are supported by widefield fluorescence microscopy observation of more DNA fibers with morphologic NET characteristics in mice with TRALI, as shown in Figure 4A by visualization of diffuse DNA structures of irregular shape (bottom left panel) and DNA streaks (bottom right panel) next to alveoli. Figure 4A also shows that this DNA probably originated from neutrophils or a subset of monocytes (Gr-1-positive, orange staining). Histone citrullination catalyzed by PAD4 (peptidylarginine deiminase 4), an enzyme prominently found in neutrophil chromatin decondensation and in NET formation.<sup>8</sup> Multiphoton analysis of fixed lung tissue allowed us to observe areas with robust citrullinated histone H3 staining colocalizing with DNA streaks in the alveoli outside blood vessels in mice with TRALI (Figure 4B right panel, C; supplemental Videos 1-2). Thus, the extracellular DNA was probably of neutrophil origin. In our model, depletion of Gr-1-positive cells prevented the appearance of hypercitrullinated histone H3 formation in the lungs of the mice subjected to TRALI, whereas platelet depletion did not preclude the presence of these NET biomarkers in the lungs (data not shown). The robust staining for citrullinated histone H3 observed in mice with TRALI was rarely present in LPS only-treated mice (Figure 4B left panel) and could not be detected by widefield fluorescence microscopy in control lungs (supplemental Figure 3).

**Table 1. Evidence of circulating NET biomarkers in serum of patients with TRALI**

Sample no.	GAT	DNA, ng/mL	MPO, mU/mL	Nucleosomes (OD 405-490)
<b>Specificity</b>				
TRALI patient 1	±	479	360.7	0.11
TRALI patient 2	±	473	270.8	0.40
TRALI patient 3	±	270	112.4	0.20
TRALI patient 4	±	523	466.5	0.50
TRALI patient 5	±	522	55.5	0.11
Group median		479	270.8	0.20
Normal control 1	–	266	39.7	0
Normal control 2	–	294	79.6	0.01
Normal control 3	–	250	45.9	0.06
Normal control 4	–	221	243	0.10
Normal control 5	–	241	87.4	0.07
Normal control 6	–	235	138.9	0.05
Group median		245	83.5	0.06
<i>P</i>		.0087	.1255	.0043

The degree of agglutination was graded from – (negative), ± (weak), or + (positive). DNA, MPO, and nucleosome levels are compared in serum from patients with TRALI with control serum ( $P = .0087$ , .1255, and .0043, respectively). Analysis was performed blinded to sample origin. All the TRALI patients' samples were higher than all control samples for at least 1 biomarker.

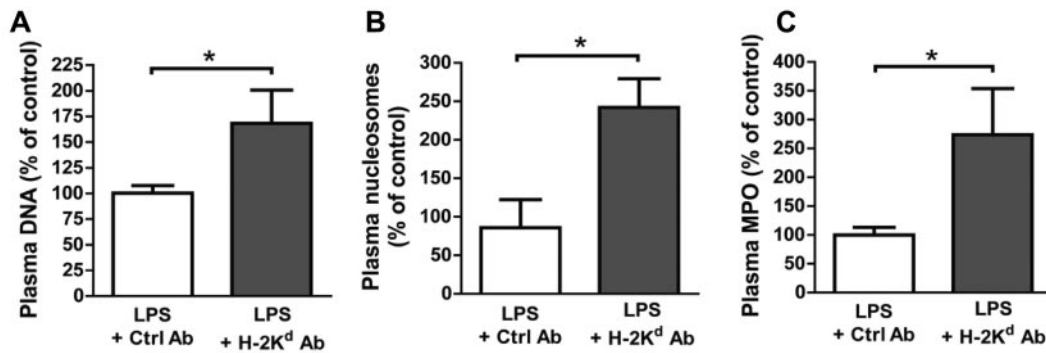


**Figure 2. Evidence of circulating NET biomarkers in the mouse model of TRALI.** Quantification of (A) DNA, (B) nucleosomes, and (C) MPO concentrations in plasma from a group of mice challenged intraperitoneally with LPS (0.1 mg/kg) and intravenously with an isotype control antibody (1 mg/kg; LPS + Ctrl Ab);  $n = 7, 7,$  and  $4$  for panels A, B, and C, respectively), and from a TRALI group that received both LPS and the anti-H-2K<sup>d</sup> antibody (1 mg/kg; LPS + H-2K<sup>d</sup> Ab;  $n = 7, 7,$  and  $4$  for panels A, B, and C, respectively). Blood was taken 2 hours after antibody injection. \* $P < .05$ .

### NET disruption in alveoli during TRALI can improve blood oxygenation in mice

Because intranasal DNase 1 treatment of the mice before anti-H-2K<sup>d</sup> mAb infusion can prevent NET deposition in the lungs, we examined whether it could improve lung function in mice with TRALI. Mice subjected to TRALI present transient hypoxia as shown by down spikes in blood arterial oxygenation saturation (saturation  $< 90\%$ ; Figure 5A top panel), a phenomenon not observed in control healthy mice (data not shown). These down spikes were significantly attenuated in the mice pretreated with DNase 1 (Figure 5A bottom panel) compared with the vehicle

buffer-pretreated mice. A general effect of DNase 1 on blood oxygenation can be measured and is depicted as an increase of the mean arterial oxygen saturation recorded (overall oxygen saturation stability, Figure 5B) accompanied by an increase in the minimum arterial oxygen saturation measured during the 20 minute-recording time (hypoxia episode intensity, Figure 5C) compared with healthy mice. Our results showed that DNase 1 given intranasally as a pretreatment but also given intranasally as a treatment 90 minutes after the onset of TRALI succeeded in correcting the defect in blood oxygenation observed during TRALI. Body temperatures were also monitored as a measure of the shock-like condition induced by the

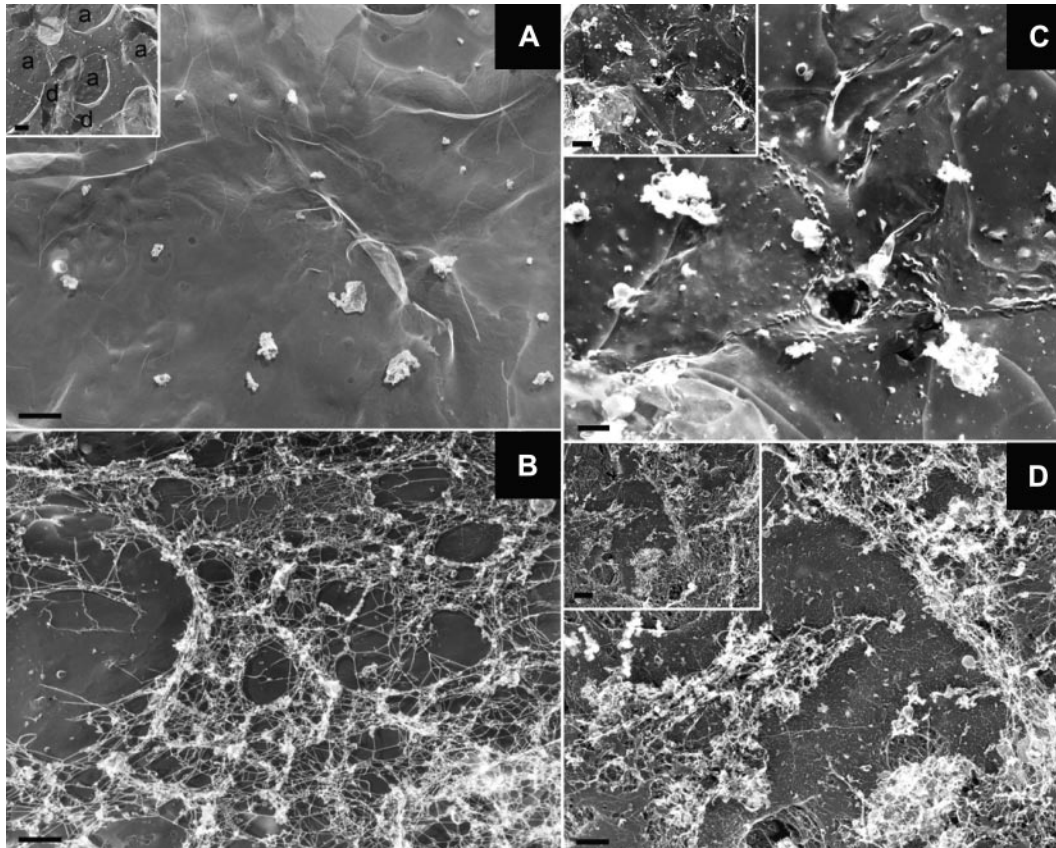


**Figure 3. A DNA-based fibrous mesh is present in the lungs of mice with TRALI.** (A-D) Representative photographs obtained by transmission electron microscopy of the lung epithelial surface of control mice (A), mice with TRALI (B,D), and mice that were injected with LPS (0.5 mg/kg) and received DNase 1 before anti-H-2K<sup>d</sup> mAb injection (C). The fibrous material found in TRALI lungs is absent after DNase 1 treatment. Scale bar represents  $1 \mu\text{m}$ . The insets show low magnification views of the lung surface revealing alveolar sacs (a) and ducts (d); inset scale bars represent  $2 \mu\text{m}$ . The pictures are representative of 3 independent experiments.



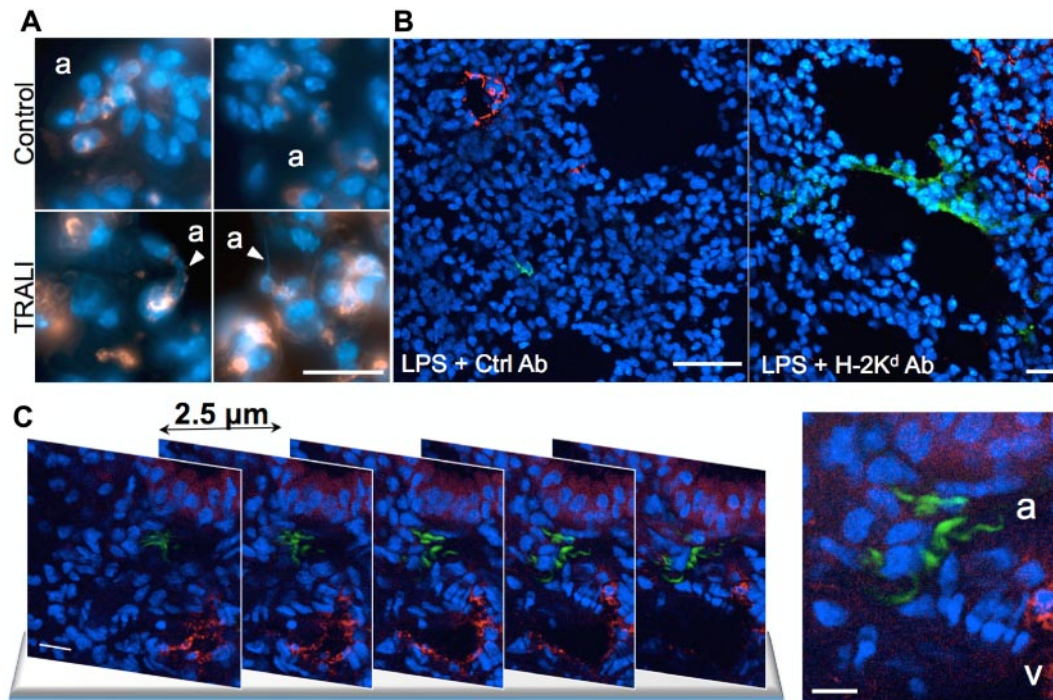


**Figure 4. NETs are formed in the lungs of mice with TRALI.** (A) Lung tissue cryosections from control healthy mice (control) and from mice with TRALI (2 hours after antibody injection, TRALI) were immunostained for Gr-1 (orange) and stained for DNA (Hoechst 33342, blue) and then observed by widefield fluorescence microscopy. White arrowheads point at NET structures probably originating from Gr-1-positive cells. a indicates alveolus. Scale bar represents 20  $\mu$ m. (B) Multiphoton fluorescence micrographs of a lung tissue cryosection from an LPS-treated mouse (LPS + Ctrl Ab) and from a mouse with TRALI (LPS + H-2K<sup>d</sup> Ab). The sections were immunostained for VWF (red) to show blood vessels, histone H3Cit (green), and counterstained for DNA (Hoechst 33342, blue). Three independent experiments were immunostained. Scale bars represent 200  $\mu$ m. (C) Multiphoton fluorescence micrographs of lung tissue cryosections from a mouse with TRALI. Five representative sequential sections 2.5  $\mu$ m apart are shown. Tissue cryosections were stained as in panel B. v indicates vessel. Scale bars represent 10  $\mu$ m. The z-stack and the 3-dimensional reconstruction of the specimen are online as supplemental Videos 1 and 2.

LPS/anti-H-2K<sup>d</sup> mAb infusion. Although the mice with TRALI were showing signs of hypothermia 2 hours after mAb infusion (Figure 5D), rectal temperatures were normal in mice subjected to TRALI and that received DNase 1 either as prophylaxis or treatment. These results support the hypothesis that NETs are indeed formed in TRALI lungs and are involved in the pathophysiology of TRALI.

## Discussion

NETs are important in antibacterial defense,<sup>6,7</sup> but several studies have shown that NETs<sup>31</sup> and their components, such as histones,<sup>12,32</sup> elastase,<sup>11</sup> or pentraxin-3,<sup>13</sup> are injurious to tissues. Histones, at a high dose, can even induce death when infused intravenously in mice.<sup>12,16</sup> In addition, NETs activate blood coagulation<sup>33</sup> and platelets.<sup>29,34</sup> Histone infusion causes rapid thrombocytopenia in mice,<sup>34</sup> and mild thrombocytopenia is one of the hallmarks of the mouse TRALI model<sup>20</sup> (supplemental Figure 1) where we show that NETs are generated. Reduced platelet counts have been observed during TRALI in a retrospective study of patients developing TRALI compared with controls.<sup>35</sup> Activation of platelets can, in turn, promote additional neutrophil activation and more NET generation.<sup>33,36</sup> This has been observed in a sepsis model where LPS was shown to activate platelets through TLR4, promoting platelet-neutrophil complex formation and NET generation. In addition, collagen-mediated platelet activation, such as would occur in trauma or major surgery, was linked to platelet-induced NET formation.<sup>33</sup> Interestingly, both infection and surgery are risk factors for developing TRALI.<sup>2,37,38</sup> We propose that a harmful factor, a common denominator of the different scenarios causing TRALI, could be NET formation and its injury to the lung.

Indeed, platelets have been shown to contribute to the TRALI mouse model that we used where LPS is given as a primer before antibody infusion. Looney et al have shown that, after LPS priming, antibody-induced TRALI could be prevented by platelet depletion.<sup>20</sup> A recent study using a model without LPS priming showed that platelets were not required for TRALI development.<sup>27</sup> Even if LPS-activated platelets may be involved in vascular cell activation and in NET formation, we observed that platelet depletion with neuraminidase did not prevent NET formation in the lungs of mice with TRALI. However, this result does not exclude that the presence of platelets may further augment NET formation as our analysis was only qualitative.

In most animal models, an antibody infusion is needed or is sufficient to induce TRALI. In both mouse models discussed in the preceding paragraph, Fc $\gamma$  receptor (Fc $\gamma$ R) activation was implicated in the TRALI process.<sup>26,27</sup> Silliman et al have shown in an in vitro study that Fc $\gamma$ R are not required in neutrophil-mediated damage of endothelial cells at early time points after anti-HNA-3a antibody incubation.<sup>5</sup> However, it may not be the case at later time points where Fc $\gamma$ R-binding may lead to NET formation in the lungs during TRALI. The question of whether Fc $\gamma$ R are involved or not in mouse TRALI was first asked by Looney et al.<sup>26</sup> They have shown that Fc $\gamma$ R<sup>-/-</sup> mice were protected from TRALI after anti-H-2K<sup>d</sup> antibody challenge and observed that the injection of wild-type neutrophils into Fc $\gamma$ R<sup>-/-</sup> mice restored ALI after mAb delivery. Strait et al recently reported that Fc $\gamma$ R were playing a role in TRALI but that they were not responsible for all the lung injury and that macrophages and complement activation were also involved.<sup>27</sup>

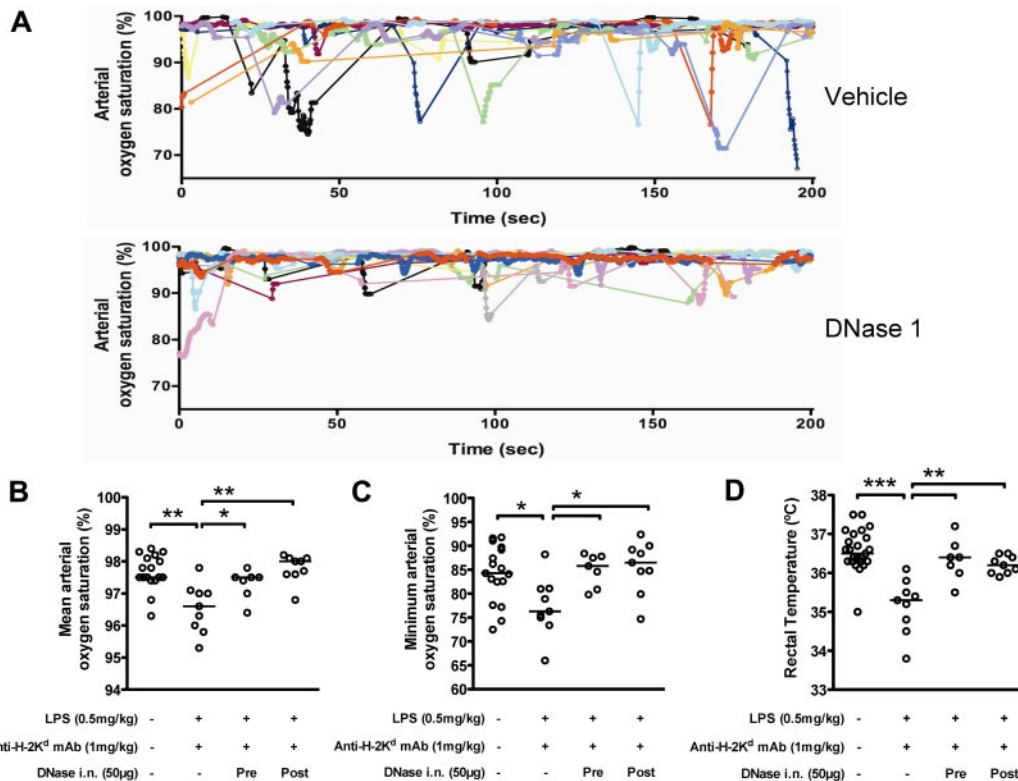


**Figure 5. DNase 1 treatment improves blood oxygenation of mice with TRALI.** (A) Examples of individual arterial blood oxygen saturation curves recorded in mice with TRALI. The mice received (top panel) intranasal vehicle buffer (n = 11 mice) or (bottom panel) intranasal DNase 1 (n = 11 mice) 10 minutes before anti-H-2K<sup>d</sup> antibody injection. Mice that received DNase 1 showed more stable arterial blood oxygen saturation and improved transient hypoxia compared with the mice pretreated with the vehicle buffer. (B-C) Mean (B) and minimum (C) of the arterial oxygen saturation recorded for 20 minutes 2 hours after antibody infusion in control mice (n = 17), mice with TRALI (n = 9), mice with TRALI that have received DNase 1 as a pretreatment 10 minutes before antibody infusion (n = 7; Pre) or as a treatment 90 minutes after antibody infusion (n = 9; Post). Mice with TRALI received intranasally either the vehicle buffer or DNase 1. Bars represent medians. \**P* < .05. \*\**P* < .01. (D) Shock-like condition was determined by rectal temperature measurement in the mice monitored for arterial oxygen saturation and additional control mice (control group: n = 25). Bars represent medians. \*\**P* < .01. \*\*\**P* < .005.

In our current study, we demonstrated that human TRALI-inducing antibodies stimulated NET generation from primed human neutrophils and this required the Fc portion of the antibody. Just crosslinking of the neutrophil antigen/receptor HNA-3a/CTL-2 was not sufficient to activate NET formation because we observed that anti-HNA-3a F(ab')<sub>2</sub> fragment-treatment on TNF-α-primed neutrophils did not induce NET generation. Thus, NET initiation by the antibody probably also implicates a FcγR binding-dependent mechanism. Furthermore, when TNF-α-primed human neutrophils were treated with another antibody that binds neutrophils, more NETs were observed compared with treatment with an isotype control antibody (G.M.T. and D.D.W., unpublished data, January 14, 2011). Thus, we propose a specific mechanism ultimately leading to NET formation in antibody-mediated TRALI through FcγR activation. Our data are consistent with studies describing NET production in autoimmune diseases such as small-vessel vasculitis<sup>14</sup> or systemic lupus erythematosus,<sup>15,39</sup> where FcγR can be activated.<sup>24,40,41</sup>

However, NETs may be formed in nonantibody-mediated TRALI as well. No antibodies could be detected in the transfused units to 2 of the 5 TRALI patients examined in this study, and yet NET biomarkers were generated and could be detected in their circulation (supplemental Table 1; Table 1). In 1997, Silliman et al proposed that biologically active lipids released during blood storage could activate neutrophils and cause TRALI.<sup>37,42</sup> Other groups have also reported effects of components present and accumulating in the supernatant of stored platelets on neutrophil activation both in vitro and in animal models.<sup>2,22,43-45</sup> A recent study

showed that longer platelet storage was associated with an increased risk of TRALI in patients.<sup>46</sup> One such biologically active lipid that could be formed during platelet storage, platelet-activating factor, is a good inducer of NET formation in vitro,<sup>29</sup> and other biologically active lipids could be as well. Similarly, NETs can form in ALI,<sup>32,47</sup> in which released cytokines or bacterial presence have already been described as strong NET inducers.<sup>6,13,48</sup> Thus, it is possible that a variety of stimulants implicated in TRALI may alone or in combination with another “hit” induce NET formation.

Lungs may be the most susceptible organ for NET deposition after transfusion, as clumped activated neutrophils would probably be trapped in lung microcirculation and transmigrate locally while forming NETs. However, the degradation products of NETs were found systemically in blood of both patients and mice with TRALI. These are probably generated by DNase 1, which is present in the plasma of mice and humans and whose function is to degrade DNA released from dying cells.<sup>49</sup> Indeed, there is no certainty that the increase in NET biomarkers measured in human blood from TRALI patients is the result of only the TRALI reaction. That is why additional data were provided to show that NETs are formed in vitro by neutrophils in response to the HNA-3a antineutrophil antibody challenge, and in vivo in the lungs and plasma of originally healthy mice with TRALI. Recently, we have shown that supplementing mice intravenously with DNase 1 prevented NET-initiated thrombosis in a mouse model of deep vein thrombosis<sup>50</sup> and reduced brain injury in a mouse model of stroke.<sup>51</sup> In this mouse TRALI model, NETs were revealed in the lung tissue by

their irregular patterns when stained for both DNA and citrullinated histones, a hallmark of NET generation (Figure 4; supplemental Figure 3) and their DNA bases confirmed by DNase 1 susceptibility (Figure 3). Somewhat surprisingly to us, NETs were found in abundance in the TRALI-affected alveoli with only a few detectable in the pulmonary microcirculation. The cause for NET accumulation at the alveolus interface will require further study. Either they are more protected there from plasma DNase 1 digestion and therefore are easily detected or they preferentially form at this location. Monocytes/macrophages were also shown to be important in the development of mouse TRALI.<sup>27</sup> These cells, in the alveoli, together with lung epithelial cells, generate lung inflammatory mediators, such as IL-1 $\beta$  and TNF- $\alpha$ ,<sup>52</sup> both important NET inducers.<sup>14,17</sup> These 2 cytokines could provide a strong local stimulus to the neutrophils primed in the vessels by antibodies or bioactive lipids for NET production at this location.

Importantly, we observed that NET deposition in mouse lungs could be interrupted by DNase 1 inhalation. This treatment not only prevented NET accumulation in the alveoli but also appeared to improve the lung function of the mice experiencing TRALI. Indeed, it seems to be in the alveoli that NETs produced the most preventable damage in TRALI. In our preliminary studies, we were unable to improve TRALI outcome with intravenous DNase 1 administration, whereas the inhalation of DNase 1 that brought the drug directly to the alveoli had a positive effect both when administered before or after TRALI onset (Figure 5). These results are exciting and show that DNase 1 could be used not only as a prophylactic agent but also as a treatment for TRALI after it started.

In conclusion, our study documents that NETs form during TRALI both in humans and in mice and that NET degradation, as shown experimentally by DNase 1 inhalation, may improve the condition of mice with TRALI. Thus, we provide a new mechanistic facet in the understanding of the pathogenesis of TRALI. The likelihood that NETs are involved in the etiology of TRALI makes them a reasonable target for therapy. DNase 1, the drug we used, is FDA-approved (Pulmozyme) to treat the lungs of cystic fibrosis patients. These patients were recently shown to produce NET markers,<sup>53</sup> which were found in their sputum. It is possible that TRALI-associated NET formation could be arrested by preventing neutrophil chromatin decondensation with neutrophil elastase inhibitors<sup>54</sup> or with inhibitors to the histone-citrullinating enzyme

peptidylarginine deiminase (PAD4).<sup>8,55</sup> NET inhibitors should be further considered in TRALI for their treatment potential or as prophylaxis for patients at high risk of developing TRALI.

## Acknowledgments

The authors thank Mia Sullivan (BloodCenter of Wisconsin) and Maureen Gallant (Immune Disease Institute) for their valuable technical assistance; Leslie Silberstein, Debra Newman, and Peter Newman for helpful discussions; Alexander Savchenko and Melanie Demers for helpful comments; and Lesley Cowan for her assistance in the preparation of the manuscript.

This work was supported by National Heart, Lung, and Blood Institute of the National Institutes of Health (grant PO1 HL056949, D.D.W., J.H.H., and U.H.v.A.; grant RO1 HL041002, D.D.W.) and IDI-GlaxoSmithKline (fellowship; G.M.T.).

## Authorship

Contribution: G.M.T. designed the study, performed most of the experiments, analyzed the data, and wrote the paper; C.C. performed the granulocyte agglutination test experiments and helped to set up the TRALI model in BALB/c mice; B.R.C. provided patient material, purified antibodies, and clinical data; K.M. and I.B.M. performed the DNA/VWF/H3Cit staining and analysis by multiphoton fluorescence microscopy; D.S. and S.M.C. provided valuable technical assistance; T.A.F. initiated patient sample analysis and participated in helpful discussions; U.H.v.A. supervised the study; J.H.H. performed lung tissue preparation, observation, and analysis by transmission electron microscopy, and supervised the study; R.H.A. provided patient material and clinical data and supervised the study; and D.D.W. designed and supervised the study, analyzed data, and wrote the paper.

Conflict-of-interest disclosure: The authors declare no competing financial interests.

Correspondence: Denisa D. Wagner, Immune Disease Institute, 3 Blackfan Cir, 3rd Fl, Boston, MA 02115; e-mail: wagner@idi.harvard.edu.

## References

- Kleinman S, Caulfield T, Chan P, et al. Toward an understanding of transfusion-related acute lung injury: statement of a consensus panel. *Transfusion*. 2004;44(12):1774-1789.
- Vlaar AP, Hofstra JJ, Determann RM, et al. The incidence, risk factors, and outcome of transfusion-related acute lung injury in a cohort of cardiac surgery patients: a prospective nested case-control study. *Blood*. 2011;117(16):4218-4225.
- Davoren A, Curtis BR, Shulman IA, et al. TRALI due to granulocyte-agglutinating human neutrophil antigen-3a (5b) alloantibodies in donor plasma: a report of 2 fatalities. *Transfusion*. 2003;43(5):641-645.
- Hashimoto S, Nakajima F, Kamada H, et al. Relationship of donor HLA antibody strength to the development of transfusion-related acute lung injury. *Transfusion*. 2010;50(12):2582-2591.
- Silliman CC, Curtis BR, Kopko PM, et al. Donor antibodies to HNA-3a implicated in TRALI reactions prime neutrophils and cause PMN-mediated damage to human pulmonary microvascular endothelial cells in a two-event in vitro model. *Blood*. 2007;109(4):1752-1755.
- Brinkmann V, Reichard U, Goosmann C, et al. Neutrophil extracellular traps kill bacteria. *Science*. 2004;303(5663):1532-1535.
- Urban CF, Ermert D, Schmid M, et al. Neutrophil extracellular traps contain calprotectin, a cytosolic protein complex involved in host defense against *Candida albicans*. *PLoS Pathog*. 2009;5(10):e1000639.
- Wang Y, Li M, Stadler S, et al. Histone hypercitrullination mediates chromatin decondensation and neutrophil extracellular trap formation. *J Cell Biol*. 2009;184(2):205-213.
- Fuchs TA, Abed U, Goosmann C, et al. Novel cell death program leads to neutrophil extracellular traps. *J Cell Biol*. 2007;176(2):231-241.
- Buchanan JT, Simpson AJ, Aziz RK, et al. DNase expression allows the pathogen group A *Streptococcus* to escape killing in neutrophil extracellular traps. *Curr Biol*. 2006;16(4):396-400.
- Bless NM, Smith D, Charlton J, et al. Protective effects of an aptamer inhibitor of neutrophil elastase in lung inflammatory injury. *Curr Biol*. 1997;7(11):877-880.
- Xu J, Zhang X, Pelayo R, et al. Extracellular histones are major mediators of death in sepsis. *Nat Med*. 2009;15(11):1318-1321.
- Savchenko AS, Inoue A, Ohashi R, et al. Long pentraxin 3 (PTX3) expression and release by neutrophils in vitro and in ulcerative colitis. *Pathol Int*. 2011;61(5):290-297.
- Kessenbrock K, Krumbholz M, Schonermarck U, et al. Netting neutrophils in autoimmune small-vessel vasculitis. *Nat Med*. 2009;15(6):623-625.
- Garcia-Romo GS, Caielli S, Vega B, et al. Netting neutrophils are major inducers of type I IFN production in pediatric systemic lupus erythematosus. *Sci Transl Med*. 2011;3(73):73ra20.
- Xu J, Zhang X, Monestier M, Esmon NL, Esmon CT. Extracellular histones are mediators of death through TLR2 and TLR4 in mouse fatal liver injury. *J Immunol*. 2011;187(5):2626-2631.
- Mitroulis I, Kambas K, Chrysanthopoulou A, et al. Neutrophil extracellular trap formation is associated with IL-1 $\beta$  and autophagy-related signaling in gout. *PLoS One*. 2011;6(12):e29318.
- Curtis BR, Cox NJ, Sullivan MJ, et al. The neutrophil alloantigen HNA-3a (5b) is located on choline



- transporter-like protein 2 and appears to be encoded by an R>Q154 amino acid substitution. *Blood*. 2010;115(10):2073-2076.
19. Greinacher A, Wesche J, Hammer E, et al. Characterization of the human neutrophil alloantigen-3a. *Nat Med*. 2010;16(1):45-48.
  20. Looney MR, Nguyen JX, Hu Y, Van Ziffle JA, Lowell CA, Matthay MA. Platelet depletion and aspirin treatment protect mice in a two-event model of transfusion-related acute lung injury. *J Clin Invest*. 2009;119(11):3450-3461.
  21. Hidalgo A, Chang J, Jang JE, Peired AJ, Chiang EY, Frenette PS. Heterotypic interactions enabled by polarized neutrophil microdomains mediate thromboinflammatory injury. *Nat Med*. 2009;15(4):384-391.
  22. Looney MR, Matthay MA. Animal models of transfusion-related acute lung injury. *Crit Care Med*. 2006;34(5 Suppl):S132-S136.
  23. Hakkim A, Fuchs TA, Martinez NE, et al. Activation of the Raf-MEK-ERK pathway is required for neutrophil extracellular trap formation. *Nat Chem Biol*. 2011;7(2):75-77.
  24. Tsuboi N, Asano K, Lauterbach M, Mayadas TN. Human neutrophil Fcγ receptors initiate and play specialized nonredundant roles in antibody-mediated inflammatory diseases. *Immunity*. 2008;28(6):833-846.
  25. Xiao Z, Visentin GP, Dayananda KM, Neelamegham S. Immune complexes formed following the binding of anti-platelet factor 4 (CXCL4) antibodies to CXCL4 stimulate human neutrophil activation and cell adhesion. *Blood*. 2008;112(4):1091-1100.
  26. Looney MR, Su X, Van Ziffle JA, Lowell CA, Matthay MA. Neutrophils and their Fcγ receptors are essential in a mouse model of transfusion-related acute lung injury. *J Clin Invest*. 2006;116(6):1615-1623.
  27. Strait RT, Hicks W, Barasa N, et al. MHC class I-specific antibody binding to nonhematopoietic cells drives complement activation to induce transfusion-related acute lung injury in mice. *J Exp Med*. 2011;208(12):2525-2544.
  28. Krautgartner WD, Klappacher M, Hannig M, et al. Fibrin mimics neutrophil extracellular traps in SEM. *Ultrastruct Pathol*. 2010;34(4):226-231.
  29. Fuchs TA, Brill A, Duerschmied D, et al. Extracellular DNA traps promote thrombosis. *Proc Natl Acad Sci U S A*. 2010;107(36):15880-15885.
  30. Asaga H, Nakashima K, Senshu T, Ishigami A, Yamada M. Immunocytochemical localization of peptidylarginine deiminase in human eosinophils and neutrophils. *J Leukoc Biol*. 2001;70(1):46-51.
  31. Gupta AK, Joshi MB, Philippova M, et al. Activated endothelial cells induce neutrophil extracellular traps and are susceptible to NETosis-mediated cell death. *FEBS Lett*. 2010;584(14):3193-3197.
  32. Saffarzadeh M, Juenemann C, Queisser MA, et al. Neutrophil extracellular traps directly induce epithelial and endothelial cell death: a predominant role of histones. *PLoS One*. 2012;7(2):e32366.
  33. Massberg S, Grahl L, von Bruehl ML, et al. Reciprocal coupling of coagulation and innate immunity via neutrophil serine proteases. *Nat Med*. 2010;16(8):887-896.
  34. Fuchs TA, Bhandari AA, Wagner DD. Histones induce rapid and profound thrombocytopenia in mice. *Blood*. 2011;118(13):3708-3714.
  35. Vlaar AP, Binnekade JM, Prins D, et al. Risk factors and outcome of transfusion-related acute lung injury in the critically ill: a nested case-control study. *Crit Care Med*. 2010;38(3):771-778.
  36. Clark SR, Ma AC, Tavener SA, et al. Platelet TLR4 activates neutrophil extracellular traps to ensnare bacteria in septic blood. *Nat Med*. 2007;13(4):463-469.
  37. Silliman CC, Boshkov LK, Mehdizadehkashi Z, et al. Transfusion-related acute lung injury: epidemiology and a prospective analysis of etiologic factors. *Blood*. 2003;101(2):454-462.
  38. Gajic O, Rana R, Winters JL, et al. Transfusion-related acute lung injury in the critically ill: prospective nested case-control study. *Am J Respir Crit Care Med*. 2007;176(9):886-891.
  39. Hakkim A, Furnrohr BG, Amann K, et al. Impairment of neutrophil extracellular trap degradation is associated with lupus nephritis. *Proc Natl Acad Sci U S A*. 2010;107(21):9813-9818.
  40. Tan Sardjono C, Mottram PL, van de Velde NC, et al. Development of spontaneous multisystem autoimmune disease and hypersensitivity to antibody-induced inflammation in Fcγ receptor IIa-transgenic mice. *Arthritis Rheum*. 2005;52(10):3220-3229.
  41. Tsuboi N, Hernandez T, Li X, et al. Regulation of human neutrophil Fcγ receptor IIa by C5a receptor promotes inflammatory arthritis in mice. *Arthritis Rheum*. 2011;63(2):467-478.
  42. Silliman CC, Fung YL, Ball JB, Khan SY. Transfusion-related acute lung injury (TRALI): current concepts and misconceptions. *Blood Rev*. 2009;23(6):245-255.
  43. Wyman TH, Bjornsen AJ, Elzi DJ, et al. A two-insult in vitro model of PMN-mediated pulmonary endothelial damage: requirements for adherence and chemokine release. *Am J Physiol Cell Physiol*. 2002;283(6):C1592-C1603.
  44. Khan SY, Kelher MR, Heal JM, et al. Soluble CD40 ligand accumulates in stored blood components, primes neutrophils through CD40, and is a potential cofactor in the development of transfusion-related acute lung injury. *Blood*. 2006;108(7):2455-2462.
  45. Vlaar AP, Hofstra JJ, Kulik W, et al. Supernatant of stored platelets causes lung inflammation and coagulopathy in a novel in vivo transfusion model. *Blood*. 2010;116(8):1360-1368.
  46. Middelburg RA, Borkent B, Jansen M, et al. Storage time of blood products and transfusion-related acute lung injury. *Transfusion*. 2012;52(3):658-667.
  47. Narasaraju T, Yang E, Samy RP, et al. Excessive neutrophils and neutrophil extracellular traps contribute to acute lung injury of influenza pneumonitis. *Am J Pathol*. 2011;179(1):199-210.
  48. Gupta AK, Hasler P, Holzgreve W, Gebhardt S, Hahn S. Induction of neutrophil extracellular DNA lattices by placental microparticles and IL-8 and their presence in preeclampsia. *Hum Immunol*. 2005;66(11):1146-1154.
  49. Napirei M, Gultekin A, Kloeckl T, Moroy T, Frostegard J, Mannherz HG. Systemic lupus-erythematosus: deoxyribonuclease 1 in necrotic chromatin disposal. *Int J Biochem Cell Biol*. 2006;38(3):297-306.
  50. Brill A, Fuchs TA, Savchenko AS, et al. Neutrophil extracellular traps promote deep vein thrombosis in mice. *J Thromb Haemost*. 2012;10(1):136-144.
  51. De Meyer SF, Suidan GL, Fuchs TA, Monestier M, Wagner DD. Extracellular chromatin is an important mediator of ischemic stroke in mice [published online ahead of print May 24, 2012]. *Arterioscler Thromb Vasc Biol*. doi:10.1161/ATVBAHA.112.250993.
  52. Skerrett SJ, Liggitt HD, Hajjar AM, Ernst RK, Miller SI, Wilson CB. Respiratory epithelial cells regulate lung inflammation in response to inhaled endotoxin. *Am J Physiol Lung Cell Mol Physiol*. 2004;287(1):L143-L152.
  53. Papayannopoulos V, Staab D, Zychlinsky A. Neutrophil elastase enhances sputum solubilization in cystic fibrosis patients receiving DNase therapy. *PLoS One*. 2011;6(12):e28526.
  54. Papayannopoulos V, Metzler KD, Hakkim A, Zychlinsky A. Neutrophil elastase and myeloperoxidase regulate the formation of neutrophil extracellular traps. *J Cell Biol*. 2010;191(3):677-691.
  55. Li P, Li M, Lindberg MR, Kennett MJ, Xiong N, Wang Y. PAD4 is essential for antibacterial innate immunity mediated by neutrophil extracellular traps. *J Exp Med*. 2010;207(9):1853-1862.